

where  $t$  is time,  $\tau$  is a characteristic relaxation time of the material in question, and  $\beta$  is a parameter (sometimes denoted the Kohlrausch exponent) that has a value between 0 and 1. Many microscopic models of transport in distributed systems (e.g., electron hopping, dipole fluctuation) have shown to result in Kohlrausch dependences of macroscopic observables.

In general, whichever model is used, the DC electrical resistivity of a material sample subjected to long-term charge-decay measurements is calculated from parameters used to fit the model to the measurement data. Various methods that

have been used to fit simplistic macroscopic models to measurement data involve large numbers of fitting parameters and involve user-dependent fitting calculations. In contrast, the Kohlrausch-relaxation-based model involves the minimum possible number of fitting parameters, and the associated fitting calculations are not user-dependent.

The applicability of the present model and its superiority to the prior macroscopic model have been demonstrated through the closeness with which this model has been shown to fit experimental data on normalized charge over 5 to 6 orders of magnitude in time (for exam-

ple, see figure). Although the validity of DC-resistivity values derived from fitting parameters of this model has yet to be demonstrated, the mere fact that these resistivity values differ from those obtained by application of the prior macroscopic model to the same experimental data indicates the need for further research to answer the questions of what are the relevant properties of the affected materials and what are the proper methods of determining these properties.

*This work was done by Mihail Petkov of Caltech for NASA's Jet Propulsion Laboratory. For more information, contact iaoffice@jpl.nasa.gov. NPO-44868*

## Sub-Aperture Interferometers

**Multiple target sub-beams are derived from the same measurement beam.**

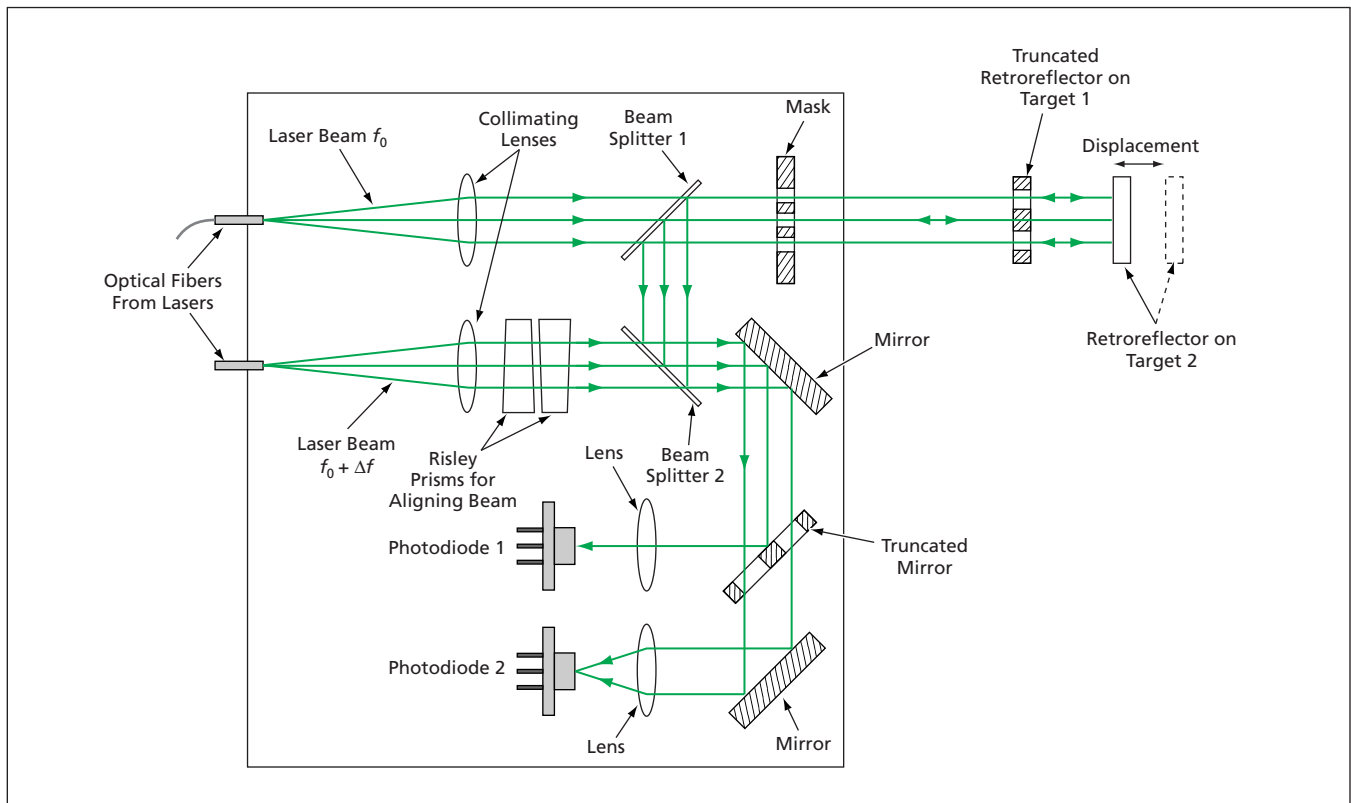
*NASA's Jet Propulsion Laboratory, Pasadena, California*

Sub-aperture interferometers — also called wavefront-split interferometers — have been developed for simultaneously measuring displacements of multiple targets. The terms “sub-aperture” and “wavefront-split” signify that the original measurement light beam in an

interferometer is split into multiple sub-beams derived from non-overlapping portions of the original measurement-beam aperture. Each measurement sub-beam is aimed at a retroreflector mounted on one of the targets. The splitting of the measure-

ment beam is accomplished by use of truncated mirrors and masks, as shown in the example below.

Sub-aperture interferometers incorporate some of the innovations described in two previous *NASA Tech Briefs* articles: “Common-Path Heter-



In this **Wavefront-Split Interferometer**, the truncated retroreflector on the first target and the retroreflector on the second target form a measurement optical cavity. The roles played by the measurement and reference beams in a typical prior interferometer are here played by two measurement sub-beams derived from the same measurement beam without use of extra optics.

odyne Interferometers” (NPO-20786), Vol. 25, No. 7 (July 2001), page 12a. and “Interferometer for Measuring Displacement to Within 20 pm” (NPO-21221), Vol. 27, No. 7 (July 2003), page 8a. Wavefront splitting is one of those innovations. To recapitulate from the second-mentioned article: Heretofore, the most popular method of displacement-measuring interferometry has involved two beams, the polarizations of which are meant to be kept orthogonal upstream of the final interference location, where the difference between the phases of the two beams is measured. Polarization leakage (deviations from the desired perfect orthogonality) contaminates the phase measurement with cyclic nonlinear errors. The advantage afforded by wavefront splitting arises from the fact that one does not utilize polarization in the separation and combination of the interfering beams; the cyclic nonlinear errors are much smaller because the polarization-leakage contribution is eliminated.

One example of a sub-aperture interferometer, denoted a sub-aperture vertex-to-vertex interferometer, is one of several prototype common-path heterodyne interferometers designed and built at NASA’s Jet Propulsion Laboratory. This interferometer (see figure) makes use of two collimated laser beams — one at a frequency of  $f_0$ , the other at the slightly different frequency of  $f_0 + \Delta f$ . The  $f_0$  beam is denoted the measurement beam. It passes through beam splitter 1 on its way toward two targets. The retroreflector on the first target is truncated; it is a flat mirror that reflects a portion of the measurement beam and contains two holes through which portions of the measurement beam continue toward the second target and through which they return after reflection from the retroreflector on the second target. A mask establishes guard bands between the measurement sub-beams to reduce diffraction.

The measurement sub-beams returning from the targets are reflected from beam splitter 1 to beam splitter 2,

where the  $f_0 + \Delta f$  beam becomes superimposed upon them. Then by use of mirrors (one of which is truncated) and lenses, the  $f_0$  sub-beam from target 1 and part of the  $f_0 + \Delta f$  beam are sent to photodiode 1 while the  $f_0$  sub-beam from target 2 and another part of the  $f_0 + \Delta f$  beam are sent to photodiode 2. The lowest-frequency components of the heterodyne outputs of the two photodetectors are signals of frequency  $\Delta f$ . The difference between the phases of these heterodyne signals is proportional to the difference between the lengths of the optical paths to the two target retroreflectors. Any displacement of either target along the optical path results in a proportional change in this phase difference. Hence, measurement of the phase difference and of any change in the phase difference yields information on the displacement.

*This work was done by Feng Zhao of Caltech for NASA’s Jet Propulsion Laboratory. For more information, contact [iaoffice@jpl.nasa.gov](mailto:iaoffice@jpl.nasa.gov). NPO-30779*

## Terahertz Mapping of Microstructure and Thickness Variations

**Previously, it was not possible to separate microstructural and thickness effects using electromagnetic methods.**

*John H. Glenn Research Center, Cleveland, Ohio*

A noncontact method has been devised for mapping or imaging spatial variations in the thickness and microstructure of a layer of a dielectric material. The method involves (1) placement of the dielectric material on a metal substrate, (2) through-the-thickness pulse-echo measurements by use of electromagnetic waves in the terahertz frequency range with a raster scan in a plane parallel to the substrate surface that do not require coupling of any kind, and (3) appropriate processing of the digitized measurement data.

More specifically, the method provides for mapping, in a coordinate system defined by the raster scan, of spatial variations of the thickness normal to the substrate surface and spatial variations of the through-the-thickness velocity of the terahertz mapping signal. (In general, variations in the velocity of this or any signal through a material are associated with variations in density and/or other characteristics associated with local microstructure of the material.) The method has been demonstrated on

nominally flat metal-backed specimens of two dielectric materials: a silicon nitride ceramic and a spray-on foam of the type used on the external tanks of a space shuttle. The method should also be applicable to other dielectric materials, and it may be feasible to extend the method to cylindrical, beveled, and other non-planar shapes.

In a prior method of terahertz mapping or imaging of this type as applied to space-shuttle external-tank foam bonded to the metal tank surface, one maps variations in the time of flight of the terahertz signal through the thickness of the foam, the time of flight being typically defined as the time between the echo from the substrate surface and the front foam surface. That approach yields information on the combined effects of thickness and through-the-thickness velocity; it does not enable separate determination of variations in thickness and variations in velocity.

In contrast, the present method provides for generation of velocity-variation images free of thickness-variation effects

and thickness-variation images free of velocity-variation effects. In this method, terahertz pulse-echo measurements with a raster scan are made as in the prior method. The raster-scan plane is chosen so that there is a suitable air gap between the terahertz transceiver and the front surface of the dielectric material. One difference between the present and prior methods is that two sets of data are acquired: For one set, the sample is absent and the times of the echoes from the substrate alone are measured. For the other set, the dielectric sample is placed on the metal substrate and echoes from both the substrate and front surface of the dielectric are measured as in the prior method.

Another difference between the present and prior methods lies in processing of the two sets of measurement data. The processing is effected by special-purpose software that performs signal-enhancement and data-fusion functions to obtain enhanced values of the times of front-surface and substrate echoes in the presence of the dielectric sample